

FORMULATION AND DEVELOPMENT OF SILICON NANO-COMPOSITE BASED CONDUCTIVE INKS.

*Okpanachi Benjamin, Ojata Abode Harry and Jafaru Braimah

Department of Physical Science Laboratory Technology,

School of Applied and Technology, Auchu Polytechnic, Auchu, Nigeria.

Corresponding Author: benjaminokpanachi2013@gmail.co_08069077090

Abstract

This study presents the formulation and development of silicon nano-composite based conductive ink for possible screen printing of selected electronic devices. An XRD technique was employed to characterize and the result analysis showed that the particles were nano- sized Silicon nano-composite based conductive inks were formulated and developed from milled silicon nano-particle which served as the dispersed phase or filler materials and dispersed in styrene acrylic and distilled water. A modified screen-printing method was adopted for the deposition of formulated inks on ceramic substrates. Current-voltage characteristics of the printed electronic devices were obtained and employed to determine the nature of interface, behavioural responses upon voltage application, resistivity, effect mass of charge carrier, and barrier height of the conductive inks. The study revealed that the mass fraction of silicon nano-particle and styrene acrylic in ink formulation E meets the needs of additive manufacturing technology of selected electronic devices.

Keywords: Silicon Nanoparticles, Conductive Ink, Screen-printing, Printable Electronics

1.0 INTRODUCTION

Printed electronics is an emerging additive manufacturing technology that is based on printing principle, has received vast attention in recent years. Compared to conventional electronics manufacturing, printed electronics has many advantages such as speediness, flexibility, personalized customization, and low cost (Lei and Jing, 2019). Its principle involves fabrication of electronic devices and systems through transferring conductive, dielectric, semiconductor materials on the substrate with conventional method such as screen printing and inkjet printing (Cui, 2019; Gao *et al*, 2019).

Conductive inks have been under investigation in recent time due to their popularity in printed and flexible electronics. They comprise specific and unique applications that belong to a whole new level of future technology (Venkata *et al*, 2015). Conductive ink is a functional composite that is made of conductive filler, binder, solvent and additive, conductive filler plays major role in its formulation and development (Li *et al*, 2014 and Lee *et al*, 2013). A conductive filler is majorly classified into three: carbon, organic polymer, and metal (Ye, 2015).

In this study, silicon nanoparticle served as a filler material dispersed in distilled water (solvent), and styrene acrylic (binder) in the formulation and implementation of an inexpensive silicon nano-composite based conductive ink suitable for large area printing of selected electronic devices.

Since the formulation and development of silicon nano-composite was achieved, there is the need to know the

nature of its interface, conduction mechanism, behavioural respond when voltages are applied and applications in printable electronics. We employed XRD technique to characterize the behaviour of the milled silicon nanoparticle. We also employed the formulated and developed silicon nanocomposite-based ink to screen print selected electronic devices. These selected electronic devices printed were electrically characterized. The silicon nano-composite based conductive ink formulated, developed, and implemented in this research work is low cost, environmentally friendly, high performance and suitable for printable electronic applications

2.0. Experimental.

2.1 Materials and Instruments

The materials used in this study are N-type extrinsic semiconductor wafer, styrene acrylic, distilled water, ceramic substrates, silver paste, and milled silicon nano-particle. The instruments used in this experiment were an electronic balance (JY5002), designed stencil, source meter (Keithley's Series 2400), an XPERT-PRO diffractometer 7000, a DHG9109 laboratory dry oven, glass rod, mechanical milling machine and rubber squeegees

2.2 Milling of Silicon Wafer (N-Type Extrinsic Semiconductor Material)

An electronic balance (JY5002) was used to weigh five N-type silicon wafers without surface treatment and the total mass was 46g. N- type extrinsic silicon wafers were placed in a contamination free container filled with five big chrome steel balls of diameter 10 cm. The chrome steel balls were used to reduce the size of the

wafers into smaller fragment via shaking. Then silicon wafers were milled by mechanical machine for a period of 5 hours. The machine was shut down to cool. The milled silicon powders were collected from the machine. The silicon powders were stored in capillary tubes with lids. Properties of milled silicon are shown in Table 1:

Table 1. Properties of milled silicon nanoparticle s

S/N	Properties of Milled Silicon	Value
1.	Diameter	100 mm
2.	crystal orientation	<100>
3.	resistivity	0 – 100 Ωm
4.	thickness	500
5.	mass of milled silicon	46 kg

2.3 Structural Characterization of Milled Powder

An XPERT-PRO diffractometer 7000 was employed for the structural characterization of the milled silicon nanoparticle to determine its crystallite size. In this study, Debye-Scherrer model was used to calculate the crystallite or grain size, as thus:

$$T = \frac{C\lambda}{B\cos\theta} \quad (1)$$

Where T is the grain size, B is the full width at half maximum, λ is the wavelength and θ is the incidence angle or Bragg angle of the X-rays and C is the shape factor (Benjamin, 2017). The scanning angle was from 4° to 12 in order to minimize the background noise. The generator setting for powder samples employed was 40 kV (voltage), and 30mA (current). The step size for the measurement (2θ) was 0.0670 employing Cu-K α (1.54060 Å) radiation. The d-spacing of the reflecting planes and the lattice parameters were also calculated using Bragg's law and Miller indices:

$$n\lambda = 2d_{hkl}\sin\theta_{hkl} \quad (2)$$

$$d = \frac{a}{\sqrt{(h^2 + k^2 + l^2)}} \quad (3)$$

Where d is the inter-planar spacing, a is a lattice parameter and hkl is the miller indices and n is the number of atoms.

2.4 Conducting Ink Formulation

The silicon powder, styrene acrylic ratios were: 50:50, 40:60, 30:70, 20:80, and 10:90 and 10 ml of distilled water was used for all the inks. 10ml of distilled water, measured silicon powder and styrene acrylic in ratios of 50:50 was placed in a reaction vessel to be fully dissolve

and then stirred with glass rod until smooth gel was obtained. These procedures were repeated for 40:60, 30:70, 20:80 and 10:90 The smooth gels or inks obtained for each ratio was labelled as ink A (50:50), ink B (40:60), ink C (30:70), ink D (20:80), and ink E (10:90).

2.5 Deposition Method

A modified screen-printing method was adopted in which a glass rod and a rubber squeegee to force a silver paste on a ceramic substrate via a stencil pattern. The printed silver paste served as a metallic contact or an electrode. Silicon nano-composite based inks were printed in - between two silver paste electrodes on the ceramic substrate via screen printing technique after the electrodes were heated to a temperature of 150 °C in a dry oven for about 30 mins.

2.6 Sintering and Post-printing Processes

A modified screen-printing method was adopted in which a glass rod and a rubber squeegee to force a silver paste on a ceramic substrate via a stencil pattern. The printed silver paste served as a metallic contact or an electrode. Silicon nano-composite based inks were printed in - between two silver paste electrodes on the ceramic substrate via screen printing technique after the electrodes were heated to a temperature of 150 °C in a dry oven for about 30 mins.

2.7 Sintering and Post Printing Procedure

The silver paste contacts of electrodes were heated to a temperature of about 30 mins to ensure equilibration followed by curing for 30 mins and cooling. This was carried out for the different combination ratios. The entire printed electronic devices were heated to a temperature of 250°C for 15 mins to convert the formulated inks into silicon nano-composite based conductive electronic inks.

2.8 Silicon Nano-composite Based Conductive Ink Performance Test

The printed electronic device was subjected to voltage in the range of (0 – 10 V) and to measure the current, which was repeated for each of the samples.

3.0 RESULT AND DISCUSSION

3.1 XRD Analysis

Figure 1 shows the diffraction pattern for milled N-type silicon. Figure 2 shows A Gaussian function fit of the most intense peak (111) for small peak width broadening of Figure 1

The structural parameters for silicon nanoparticles obtained from X-ray diffraction pattern of analysed sample is as shown in Table 2

3.2.1 Measurement of Barrier Height

Figures 3 - 7 show I-V characteristics of the manufactured electronic devices. These plots revealed the nature of the interface. From the characteristics we were able to determine the Schottky barrier height that revealed the nature of the interface (Sze, 1985).

For 50:50

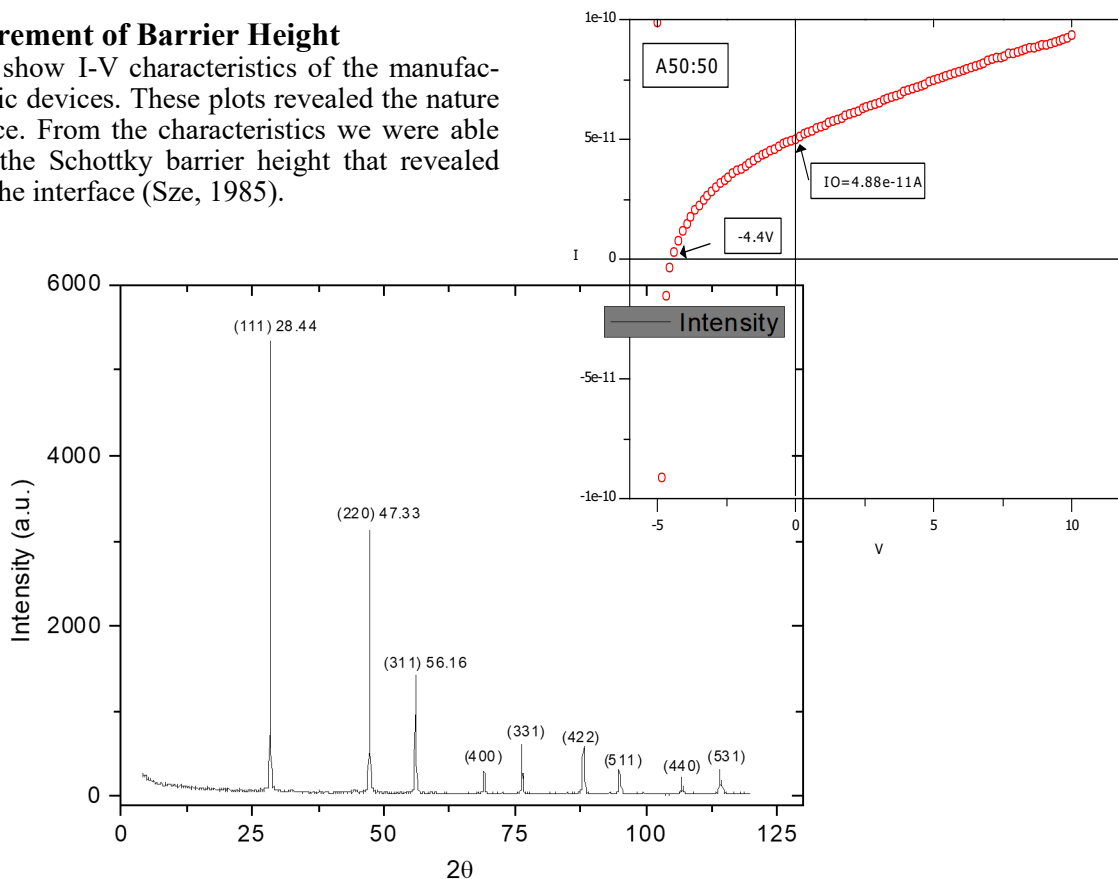


Figure 1 Actual X-Ray Diffraction pattern of Silicon.

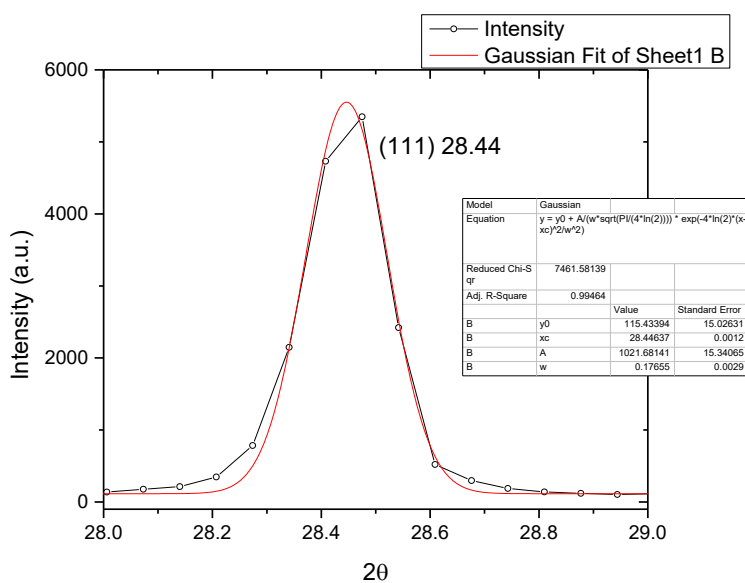


Figure 2. A Gaussian function fit of the most intense peak (111) for small peak width broadening.

Table 2. Average lattice parameter of X-ray diffraction of typical silicon

Peak #	2θ	θ	hkl	$h^2 + k^2 + l^2$	$a(A^\circ)$	$d(A^\circ)$
1	28.44	14.22	111	3	5.4332	3.1369
2	47.33	23.67	220	8	5.4264	1.9185
3	56.13	28.07	311	11	5.4295	1.6370
4	69.13	34.57	400	16	5.4306	1.3596
5	76.38	38.19	331	19	5.4310	1.2459
6	88.03	44.02	442	24	5.4309	1.1085
7	94.95	47.48	511	27	5.4307	1.0451
8	106.72	53.36	440	32	5.4306	0.9600
9	114.10	57.05	531	35	5.4309	0.9180

Average lattice parameter = 5.4304A°

Figure 3. I-V Characteristics for Printed Electronic Device A (50: 50)

Deductions from I-V characteristics

The characteristics is typically non-linear, shows clear departure from an ideal Schottky contact, at zero applied voltage current is not zero) $I_o = 4.88 \times 10^{-11} A$, and possible build-up of space charge, indicative of a depletion layer with trapped charges.

For 40:60

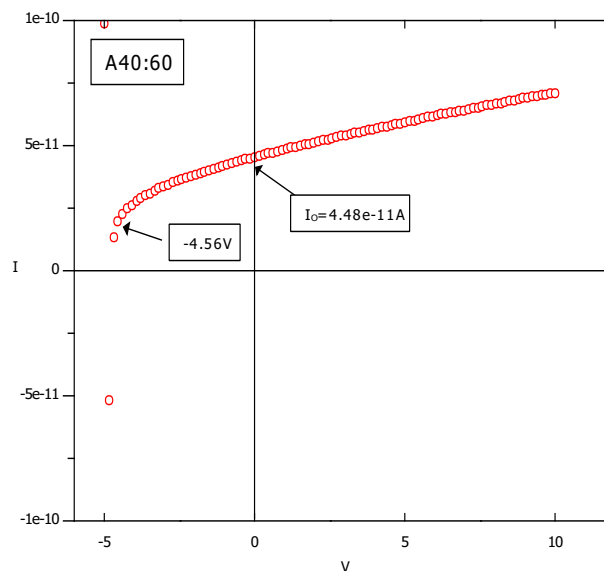


Figure 4. I-V characteristics for Printed Electronic Device B (40:60)

Deductions from I-V characteristics

The characteristics is typically non-linear, display clear departure from an ideal Schottky contact, at zero applied voltage current is not zero) $I_o = 4.48 \times 10^{-11} A$, and possi-

ble build-up of space charge, indicative of a depletion layer with trapped charges

For 30:70

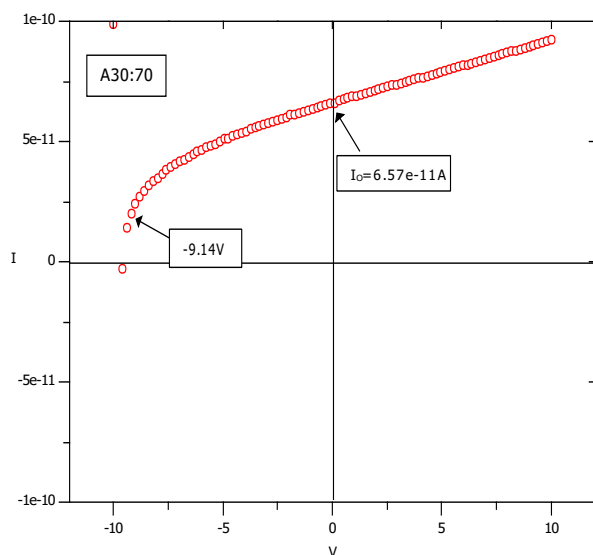


Figure 5. I-V Characteristics for Printed Electronic Device C 30:70

In Figure 5, the characteristics is non-linear, depicted a clear departure from an ideal Schottky contact, and at zero applied voltage current is not zero) $I_0 = 6.57 \times 10^{-11} A$, and possible built up of space charge, indicative of a depletion layer with trapped charges.

In Figure 6, the characteristics is also non-linear, obvious clear departure from an ideal Schottky contact, at zero applied voltage current is not zero) $I_0 = 6.52 \times 10^{-11} A$, and possible build-up of space charge, indicative of a depletion layer with trapped charge.

As shown in Figure 7, the characteristics is also non-linear, a deviation from an ideal Schottky contact, at zero applied voltage current is not zero) $I_0 = 4.89 \times 10^{-11} A$, and possible built up of space charge, indicative of a depletion layer with trapped charges. From the Figures 3 - 7, all the printed electronic devices displayed that are typically non-linear, deviated from an ideal Schottky contact.

For 20:80

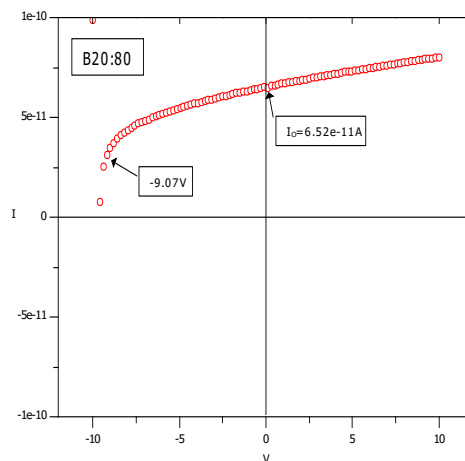


Figure 6. I-V Characteristics for Printed Electronic Device D 20:80

For 10:90

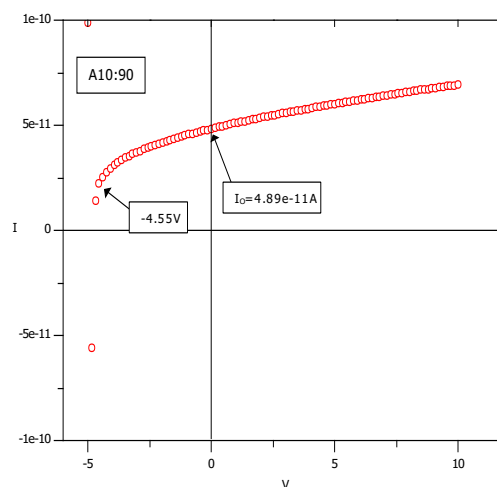


Figure 7. I-V characteristic for Printed Electronic Device (10:90)

They have leakage current that are not the same due to charges trapped in the depletion layer of the devices. Ink formulation has the lowest and stable leakage as compared with other conductive ink (Zhihui *et al.*, 2020).

3.2.1 Barrier Height Determination

Equation 4 was used to calculate the barrier height and the result as presented in Table 3.

$$I = AA^*T^2 \exp\left(-\frac{q\Phi_{B0}}{kT}\right) \exp\left[\frac{q(V - IR_s)}{kT} - 1\right] = I_s \exp\left(\frac{qV}{kT}\right) \quad (4)$$

Where V is the voltage across the Schottky diode, A is the surface contact area, A^* is the effective Richardson constant, T the temperature, ϕ_{B0} is the barrier height of the Schottky contact, q is the elementary charge, k the Boltzmann constant, R_s is its series resistance and I_s is the saturation current.

Table 3: Barrier Height of Printed Electronic Device

Printed Electronic Device	Barrier Height (cm)
A (50:50)	6.02×10^{-40}
B (40:60)	6.29×10^{-40}
C (30:70)	8.51×10^{-40}
D (20:80)	4.10×10^{-40}
E (10:90)	5.51×10^{-40}

The calculated barrier heights of the samples are as shown in Table 3. It can be seen from the Table 3 that as the mass fraction of silicon nanoparticle increased and that of styrene acrylic decreased, the barrier height in the junction (silicon nanocomposite) decreased.

3.2.2 The Effective Mass of Charge Carrier

The effective mass of the charge carrier was calculated using Equation 5 and the result is presented in Table 4,

$$I_{FN} = AE^2 \exp\left(-\frac{B}{E}\right) \quad A = \frac{q^3}{16\pi^2 \hbar m^* \phi} \quad \text{and}$$

$$B = \frac{4\sqrt{2}m^* \phi^{3/2}}{3q\hbar} \quad (5)$$

Table 4. The Results of Effective Mass of the Charge Carrier

Printed Electronic Device	Effective Mass of Charge Carrier (kg)
A (50:50)	1.42×10^{-13}
B (40:60)	1.39×10^{-13}
C (30:70)	9.64×10^{-12}
D (20:80)	2.07×10^{-12}
E (10:90)	1.40×10^{-12}

The Table 4 showed that the smaller the effective mass of the charge carrier, the lower the barrier height at the Junction between the silver paste contacts.

3.2.3 Measurement of Resistivity of Silicon Nano-composite Based Conductive Ink

The resistances of the printed samples were measured using multi-meter, the resistivity was calculated using the equation (6) and the result is presented in Table 5.

$$\rho = \frac{RA}{l} \quad (6)$$

Table 5. The results of Resistivity

Printed Electronic Device	Resistance(Ω)	Resistivity (Ωm)
A (50:50)	6.58	13.15
B (40:60)	5.75	11.50
C (30:70)	5.35	10.76
D (20:80)	5.15	10.30
E (10:90)	5.05	10.10

It can be seen from Table 5 that as the silicon nanoparticles increased compared to that of styrene acrylic in ratio 10: 90 (ink E), the resistivity of the ink decreased gradually and conductivity gradually increased

3.3 Discussions

3.3.1. X-ray Powder Diffraction

The X-ray diffraction pattern for milled N-type silicon nano-particle is shown in Table 1. It has nine basic diffraction peaks: (111), (220), (311), (400), (331), (422), (511), (440) and (531). The different diffraction peaks are due to structural transformation from single crystal phase to polycrystalline. The most intense peak is (111) which occurred at diffraction angle of 28.4° . A Gaussian fit to the most intense peak (111) for small peak width broadening, with no indication of a broad hump indicated the presence of an amorphous phase. The determination of the full width at half maximum was carried out by this fitting thus obtained crystallite size using Equation 1. The crystallite size is calculated to be 81nm and indicated that milled silicon wafer materials are at nano-level.

From the Miller indices computation for each of the diffraction peak of the diffraction pattern in the table, they indicated that the crystal structure of the milled N-type silicon nanoparticle has diamond structure. The d-spacing of reflecting plane for each of the diffraction peak is estimated by using Equation 3 and the lattice parameter for each of the peak is depicted in Table 1. From the average lattice parameter calculated, it is inferred that the lattice

constant for silicon nanoparticles is in agreement with the lattice parameter for bulk silicon.

3.2.2 Current -Voltage Measurement

We subjected each of the printed samples to voltage application of range 0-10 V and measured the corresponding currents using source meter. The I-V characteristics plotted in this study were typically non-linear, showing clear departure from an ideal Schottky contact, at zero applied voltage, the currents through the devices were not zero, and there were possible build-up of space charges, indicative of a depletion layer with trapped charges in the developed silicon nano-composite inks.

4.0 CONCLUSION

This study revealed that as the ratio of styrene acrylic decreased and that of silicon nanoparticle increased by ratio 10:90, the lower resistivity decreased and the conductivity of the conductive inks increased. Also, as the mass ratio of the silicon nanoparticle increased, the effective mass of the charge carrier decreased, and the barrier height at the junction decreased. The conductive ink formulation E has the optimal combination for best performance with the highest conductivity, smallest effective mass of charge carrier of 1.40×10^{-15} kg, lowest resistivity of, $10.10 \Omega\text{cm}$ lowest barrier height of 5.51×10^{-40} cm at the junction, and smoothest of all formulated and developed inks.

This formulated and developed ink E in this study has good printability, low resistivity, low curing temperature, stable electrical conductivity, low barrier height, low leakage current and adhesion that meets the needs of additive manufacturing technology that is based on printing principle.

ACKNOWLEDGEMENT

We wish to express our gratitude to the Department of Physical Science Laboratory Technology, Auchu Polytechnic, Auchu, Nigeria for providing some materials and equipment used in this work.

REFERENCES

- Benjamin, O. (2017): The Study of Charge Carrier Transport in Silicon Nano-composite, M. Tech Thesis, Federal University of Technology, Akure. Nigeria.
- Cui, Z. (2019): Printing Practice for the Fabrication of Flexible and Stretchable Electronics, *Sci. China Technol. Sci.*, 62, 224-232.
- Gao, W., Ota, H., Kiriya, D., Takei, K., and Javey, A. (2019): Flexible Electronics Toward Wearable Sensing. *Acc. Chem. Res.*, 52, 523-533.
- Li, L., Ran, J., and Xin, Z. (2014): Conductive Ink and its Application Technology Progress, *Imaging Science Photochem*, 4, 393-401.
- Lee, C., Chen, C.W. (2013): Graphene Nanosheet as Ink Particle for Inject Printing On Flexible Board, *Chem Eng J*, 16, 296-302.
- Lei, W., and Jing, L. (2019): Advances in the Development of Liquid Metal Based Printed Electronic Inks, *Frontiers in materials*, 19.
- Venkata, K., Rao, R., Venkata, A.K., Karthik, P. S., and Surya, P. S. (2015): Conductive Silver Inks and their Applications in Printed and Flexible Electronics, *RSC Advances*, 95.
- Ye, L. (2015): Conductive Ink Application Status and Future Application Prospect, *Technol Inno Appl*, 19, 286.
- Zhihui, X., Li, L., Ningyu, X., Yunfei, Z., and Xin, J. (2020): Preparation and Application of Carbon-Based Conductive Ink Based on Graphene, www.Researchgate.net.